


# Dynamics of the intertropical convergence zone during the early Heinrich Stadial 1

Received: 23 August 2023

Fuzhi Lu<sup>1</sup>✉, Mahyar Mohtadi<sup>2,3</sup> & Francesco S. R. Pausata<sup>4</sup>

Accepted: 18 October 2024

Published online: 11 November 2024

ARISING FROM Y. Yang et al. *Nature Communications* <https://doi.org/10.1038/s41467-023-40377-9> (2023) Check for updates

Whether the Intertropical Convergence Zone (ITCZ) migrated meridionally or contracted and expanded in response to varying climate boundary conditions remains debated. Recently, Yang et al.<sup>1</sup> proposed that the ITCZ in the Indo-Asian-Australian monsoon region has contracted during the early Heinrich Stadial 1 (HS1). However, our thorough analyses of both proxy records and climate simulations consistently indicate a southward migration of the ITCZ during the early HS1. Our results contribute to a better understanding of the dynamics of the ITCZ during North Atlantic cold events.

Firstly, there are two main sources of uncertainty in paleoclimate records, i.e., proxy uncertainties and age uncertainties<sup>2</sup>. Age uncertainties are critical when investigating climate oscillations of such a short duration (e.g., 18.3–16.3 ka) and might mask or bias the timing of abrupt climate events. However, the study of Yang et al.<sup>1</sup> used a single, linearly interpolated age model without considering age uncertainties. Here we use the R package ‘rbacon’<sup>3</sup> to construct 10,000 Bayesian age-depth models for each record and perform Monte Carlo simulations<sup>2</sup> to combine both proxy and age uncertainties, which allows a robust assessment of uncertainties and variabilities in the proxy records (Supplementary Methods). Our results demonstrate that age uncertainties based on Bayesian age-depth models can be several times larger than that of radiocarbon dates, especially in between dating points (Supplementary Figs. S1 and S2). Neglecting age uncertainties and using a single age model would severely underestimate total uncertainties and may lead to inaccurate interpretation. For instance, the magnitudes of variations in some proxy records (e.g., ADM-159 and SK129-CR04) during the period 21–15 ka are smaller than total uncertainties and thus may not be significant (Supplementary Fig. S3).

Secondly, Yang et al.<sup>1</sup> cited five marine records to support a humid climate in northern low latitudes at -3–9°N during the early HS1 at -18.3–16.3 ka, opposite to a drying climate in the Asian monsoon region. However, our detailed comparison indicates that 4/5 of these records in fact exhibit a drying trend, consistent with the pattern of Asian summer monsoon as represented by the Hulu Cave  $\delta^{18}\text{O}$  record<sup>4</sup> (Supplementary Fig. S4). Our objective analyses based on the Bayesian change-point detection algorithm (Supplementary Methods) indicate that the onset of long-term increase in local seawater  $\delta^{18}\text{O}$  ( $\delta^{18}\text{O}_{\text{local}}$ )

records (and thus a drying climate) occurred at -18.8 ka for central Andaman Sea<sup>5</sup> (Fig. 1b), southern South China Sea<sup>6</sup> (Fig. 1d) and Eastern Arabian Sea<sup>7</sup> (Fig. 1e), and at -19.1 ka for Sulu Sea<sup>8</sup> (Fig. 1c), synchronous with -19.1 ka at Hulu Cave<sup>4</sup> (Fig. 1a). These  $\delta^{18}\text{O}_{\text{local}}$  changes, however, are opposite to that of core I106 reconstructed by Yang et al.<sup>1</sup>, which indicates a decreasing trend in  $\delta^{18}\text{O}_{\text{local}}$  (and thus a wetting climate) since -18.8 ka (Fig. 1g). Our correlation analyses based on all combinations of Bayesian age models (100 million pairs) further quantitatively indicate that these records are positively correlated with the Hulu record but negatively correlated with the I106 record (Fig. 1h, i). The only record supporting the result of core I106 is the XRF-based log (Fe/Ca) record from core MD06-3075 in the Davao Gulf, southern Mindanao<sup>9</sup>, which indicates a wetting trend since -18.5 ka (Fig. 1f). However, the hydroclimate of Mindanao is additionally influenced by the El Niño–Southern Oscillation and Pacific Walker circulation<sup>10</sup>. Taken together, these records do not support the existence of a wet belt in northern low latitudes during the early HS1.

Thirdly, Yang et al.<sup>1</sup> concluded arid conditions in the Southern Hemisphere during the early HS1, synchronous with those north of -9°N. However, seawater  $\delta^{18}\text{O}$  is not only controlled by rainfall and evaporation, but also by the advection of water masses (laterally or vertically) and ocean current changes. The marine records used to infer dry conditions in the Southern Hemisphere during the early HS1 by Yang et al.<sup>1</sup> lie in routes of South Java Current (GeoB10042-1), the Indonesian Throughflow (ITF) (SO217-18519, SO217-18515, MD01-2378, MD98-2165 and GeoB10069-3) and the Mozambique Current (GIK16160-3). These ocean currents flow from north to south and thus may transport saltier waters from more northerly locations, where rainfall was indeed reduced during the early HS1. The weakening and salinification of the ITF during glacial periods due to sea-level lowering and shelf exposure reduced the inflow of relatively fresh water and led to salinification of Indian Ocean<sup>11</sup>. This effect accumulated over time and might have reached a maximum during the early HS1 when deglaciation began<sup>11</sup>. The strengthening of Agulhas leakage due to southward shift in the Southern Hemisphere westerlies during the early HS1<sup>12</sup> could have also enhanced the Mozambique Current and brought more saltier water to site GIK16160-3. Notably, the stalagmite

<sup>1</sup>School of Geography and Ocean Science, Nanjing University, Nanjing, China. <sup>2</sup>MARUM-Center for Marine Environmental Sciences, University of Bremen, Bremen, Germany. <sup>3</sup>Faculty of Geosciences, University of Bremen, Bremen, Germany. <sup>4</sup>Department of Earth and Atmospheric Sciences, University of Quebec in Montreal, Montreal, QC, Canada. ✉e-mail: [geolfz@163.com](mailto:geolfz@163.com)

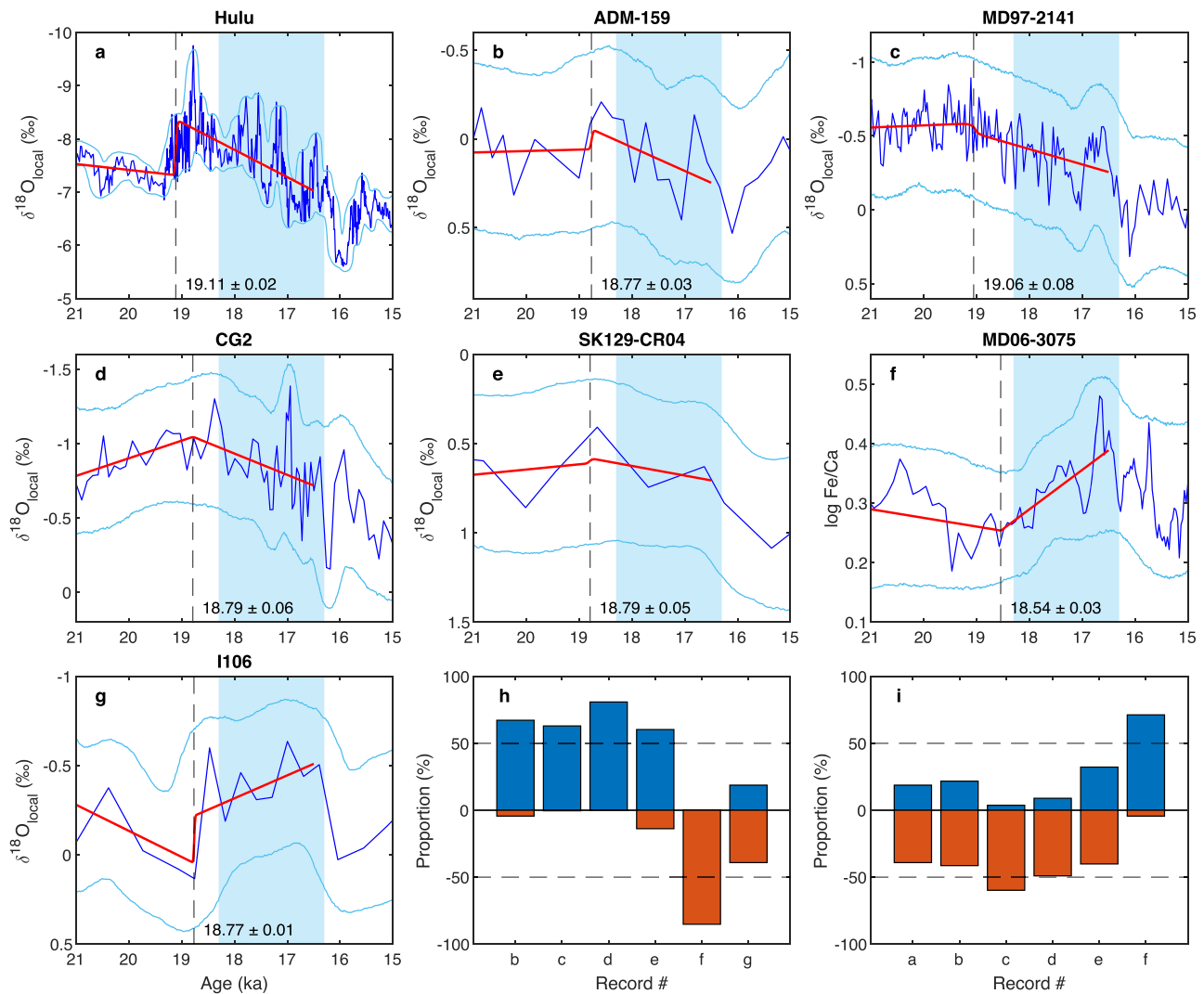


**Fig. 1 | Proxy records (blue lines) with 95% confidence interval (light blue lines) reflecting both proxy and age uncertainties. a** Stalagmite  $\delta^{18}\text{O}_{\text{local}}$  record from cave Hulu in southern China<sup>4</sup>. **b** Seawater  $\delta^{18}\text{O}_{\text{local}}$  record from core ADM-159 in central Andaman Sea<sup>5</sup>. **c** Seawater  $\delta^{18}\text{O}_{\text{local}}$  record from core MD97-2141 in Sulu Sea<sup>8</sup>. **d** Seawater  $\delta^{18}\text{O}_{\text{local}}$  record from core CG2 in southern South China Sea<sup>6</sup>. **e** Seawater  $\delta^{18}\text{O}_{\text{local}}$  record from core SK129-CR04 in Eastern Arabian Sea<sup>7</sup>. **f** XRF record of  $\log(\text{Fe}/\text{Ca})$  from core MD06-3075 in Davao Gulf<sup>9</sup>. **g** Seawater  $\delta^{18}\text{O}_{\text{local}}$  record from core

I106 in southern Bay of Bengal reported by Yang et al.<sup>1</sup>. **h** Proportions of statistically significant ( $P < 0.001$ ) positive (blue) and negative (red) correlations between Hulu record and other records. **i** Same as **h**, but for the correlations with I106 record. The red lines are piecewise linear trends of proxy records based on Bayesian change-point analysis (Supplementary Methods). The vertical dash lines with labels indicate timings of change-points in proxy records. The shading indicates the early HS1 at -18.3–16.3 ka.

$\delta^{18}\text{O}$  records from southern Indonesia<sup>13</sup> and northern Australia<sup>14</sup> and a leaf wax hydrogen isotope record offshore Zambesi River mouth<sup>15</sup> without such flaws clearly indicate higher rainfall during the early HS1.

Lastly, a contracted ITCZ during the early HS1 when the Atlantic Meridional Overturning Circulation (AMOC) weakened is not supported by global temperature reconstructions and climate model simulations. Paleoclimate data assimilation indicates cooling of the Northern Hemisphere and warming of the Southern Hemisphere during the early HS1, reducing interhemispheric temperature gradient, and the Southern Hemisphere was warmer than the Northern Hemisphere<sup>16</sup> (Supplementary Fig. S5). According to the theory of atmospheric energy balance<sup>17</sup>, the atmosphere has to compensate for the interhemispheric energy imbalance by shifting the ITCZ towards the warmer Southern Hemisphere and transfer energy via eddies and the Hadley circulation to the cooler Northern Hemisphere<sup>17</sup>. The hydroclimate records in the Indo-Asian-Australian monsoon region are significantly ( $P < 0.001$ ) correlated with the interhemispheric temperature gradient and show opposite signs between northern and

southern sites, supporting a southward migration of the ITCZ during the early HS1 (Supplementary Fig. S6). Consistent with proxy records and expectation from atmospheric energy balance, our analysis of the TraCE-21ka simulation<sup>18</sup> indicates that the ITCZ migrated into the Southern Hemisphere during the early HS1 (Supplementary Fig. S5), with rainfall decrease over the Asian monsoon region, Arabian Sea, equatorial and northern Indian Ocean, equatorial Africa, Sumatra Island, Sunda Shelf and South China Sea, and increase over southeastern Africa, southern Indian Ocean, southern Indonesia and northern Australia (Fig. 2).

In summary, our analyses reveal several issues that challenge the hypothesis of a contracted ITCZ during the early HS1 proposed by Yang et al.<sup>1</sup>. (1) Age model uncertainties have not been quantified and changes in some proxy records may be not significant. (2) The majority of proxy records do not indicate a narrow, wet hydrological belt in the northern low latitudes during the early HS1. (3) The seawater  $\delta^{18}\text{O}$  records affected by advection may not be a reliable indicator of changes in local rainfall, while other rainfall proxy records have been

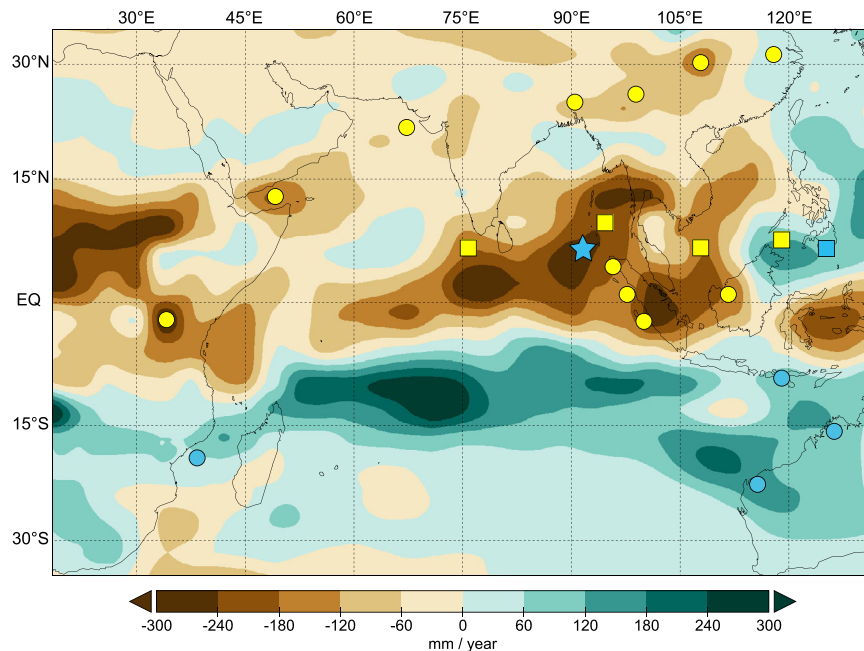


**Fig. 2 | Model-proxy comparison showing rainfall response to the weakening of the AMOC during the early HSI.** Annual rainfall difference between 17 ka and 20 ka (100 years for each period) is calculated based on the TraCE-21ka transient simulation<sup>18</sup> (shading). The blue star indicates core II06 with humid climate during the early HSI reported by Yang et al.<sup>1</sup>. The yellow (blue) circles indicate proxy

records with decreasing (increasing) rainfall during the early HSI. The yellow squares indicate marine records cited by Yang et al.<sup>1</sup> to support humid conditions in the northern low latitudes during the early HSI, which in fact indicate a drying climate. The blue square indicates core MD06-3075 in Davao Gulf<sup>9</sup> with increasing rainfall during the early HSI.

neglected. (4) Global temperature reconstructions and climate simulations indicate a southward migration of the ITCZ during the early HSI due to cooling of the Northern Hemisphere and warming of the Southern Hemisphere. Our study underscores the importance of considering age model uncertainties and using quantitative methods in identifying spatiotemporal pattern of change in paleoclimate records and provides a paradigm for such analyses.

### Data availability

Paleoclimate data analyzed in this study are available in the original references. TraCE-21ka simulation is available at <https://www.earthsystemgrid.org/project/trace.html>. Source data are provided with this paper.

### Code availability

The R package ‘rbacon’ is available at <https://cran.r-project.org/web/packages/rbacon/index.html> and example codes for Bayesian age modeling are provided in the supplementary information. The code for Bayesian change-point analysis is available in GitHub at <https://github.com/zhaokg/Rbeast>.

### References

1. Yang, Y. et al. A contracting intertropical convergence zone during the early Heinrich Stadial 1. *Nat. Commun.* **14**, 4695 (2023).
2. Shakun, J. D. et al. Global warming preceded by increasing carbon dioxide concentrations during the last deglaciation. *Nature* **484**, 49–54 (2012).
3. Blaauw, M., Christen, J. A., Bennett, K. D. & Reimer, P. J. Double the dates and go for Bayes—impacts of model choice, dating density and quality on chronologies. *Quat. Sci. Rev.* **188**, 58–66 (2018).
4. Wu, J., Wang, Y., Cheng, H. & Edwards, L. R. An exceptionally strengthened East Asian summer monsoon event between 19.9 and 17.1 ka BP recorded in a Hulu stalagmite. *Sci. China D Earth Sci.* **52**, 360–368 (2009).
5. Liu, S. et al. Paleoclimatic responses in the tropical Indian Ocean to regional monsoon and global climate change over the last 42 kyr. *Mar. Geol.* **438**, 106542 (2021).
6. Huang, J., Wan, S., Li, A. & Li, T. Two-phase structure of tropical hydroclimate during Heinrich Stadial 1 and its global implications. *Quat. Sci. Rev.* **222**, 105900 (2019).
7. Mahesh, B. S. & Banakar, V. K. Change in the intensity of low-salinity water inflow from the Bay of Bengal into the Eastern Arabian Sea from the Last Glacial Maximum to the Holocene: Implications for monsoon variations. *Palaeogeogr. Palaeoclimatol. Palaeoecol.* **397**, 31–37 (2014).
8. Rosenthal, Y., Oppo, D. W. & Linsley, B. K. The amplitude and phasing of climate change during the last deglaciation in the Sulu Sea, western equatorial Pacific. *Geophys. Res. Lett.* **30**, 1428 (2003).
9. Fraser, N. et al. Precipitation variability within the West Pacific Warm Pool over the past 120 ka: Evidence from the Davao Gulf, southern Philippines. *Paleoceanography* **29**, 1094–1110 (2014).
10. Stott, L., Poulsen, C., Lund, S. & Thunell, R. Super ENSO and global climate oscillations at millennial time scales. *Science* **297**, 222–226 (2002).
11. Nuber, S. et al. Indian Ocean salinity build-up primes deglacial ocean circulation recovery. *Nature* **617**, 306–311 (2023).
12. Dyez, K. A., Zahn, R. & Hall, I. R. Multicentennial Agulhas leakage variability and links to North Atlantic climate during the past 80,000 years. *Paleoceanography* **29**, 1238–1248 (2014).
13. Ayliffe, L. K. et al. Rapid interhemispheric climate links via the Australasian monsoon during the last deglaciation. *Nat. Commun.* **4**, 2908 (2013).
14. Denniston, R. F. et al. A Last Glacial Maximum through middle Holocene stalagmite record of coastal Western Australia climate. *Quat. Sci. Rev.* **77**, 101–112 (2013).
15. Schefuß, E., Kuhlmann, H., Mollenhauer, G., Prange, M. & Pätzold, J. Forcing of wet phases in southeast Africa over the past 17,000 years. *Nature* **480**, 509–512 (2011).

16. Osman, M. B. et al. Globally resolved surface temperatures since the Last Glacial Maximum. *Nature* **599**, 239–244 (2021).
17. Schneider, T., Bischoff, T. & Haug, G. H. Migrations and dynamics of the intertropical convergence zone. *Nature* **513**, 45–53 (2014).
18. Liu, Z. et al. Transient simulation of last deglaciation with a new mechanism for Bølling-Allerød warming. *Science* **325**, 310–314 (2009).

## Acknowledgements

We thank J. Y. Zhao, D. L. Chen, and Z. Y. Liu for helpful discussions to improve this study. F.Z.L. was supported by the National Key R&D Program of China (grant no. 2023YFF0804700) and the Innovation and Creativity Research Program of Nanjing University (grant no. CXC19-54).

## Author contributions

F.Z.L. conceived the study and analyzed the data. F.Z.L., M.M. and F.S.R.P. wrote the manuscript.

## Competing interests

The authors declare no competing interests.

## Additional information

**Supplementary information** The online version contains supplementary material available at <https://doi.org/10.1038/s41467-024-53999-4>.

**Correspondence** and requests for materials should be addressed to Fuzhi Lu.

**Peer review information** *Nature Communications* thanks the anonymous reviewer(s) for their contribution to the peer review of this work.

**Reprints and permissions information** is available at <http://www.nature.com/reprints>

**Publisher's note** Springer Nature remains neutral with regard to jurisdictional claims in published maps and institutional affiliations.

**Open Access** This article is licensed under a Creative Commons Attribution-NonCommercial-NoDerivatives 4.0 International License, which permits any non-commercial use, sharing, distribution and reproduction in any medium or format, as long as you give appropriate credit to the original author(s) and the source, provide a link to the Creative Commons licence, and indicate if you modified the licensed material. You do not have permission under this licence to share adapted material derived from this article or parts of it. The images or other third party material in this article are included in the article's Creative Commons licence, unless indicated otherwise in a credit line to the material. If material is not included in the article's Creative Commons licence and your intended use is not permitted by statutory regulation or exceeds the permitted use, you will need to obtain permission directly from the copyright holder. To view a copy of this licence, visit <http://creativecommons.org/licenses/by-nc-nd/4.0/>.

© The Author(s) 2024